

Original Article

Glomerular changes in microscopic haematuria, studied by quantitative immunoelectron microscopy and *in situ* zymography

Sawsan M. Jalalah¹, Ibrahim H. Alzahrani¹ and Peter N. Furness²

¹Department of Pathology, King Abdulaziz University, Jeddah, Saudi Arabia and ²Department of Pathology, University of Leicester, Leicester, UK

Abstract

Background. Haematuria of glomerular origin, even if mild, implies the development of defects in the glomerular basement membrane (GBM). In diseases where there is no infiltration of leukocytes into the glomerulus—such as thin basement membrane disease (TBMD) and histologically mild cases of IgA nephropathy (IgAN)—the mechanism by which such defects form is unclear.

Methods. Frozen renal tissue from 18 cases of TBMD, 18 of mild IgAN and 18 cases with no detectable abnormality were studied: (i) by quantitative *in situ* zymography, to estimate the activity of glomerular collagenases; and (ii) by quantitative immunoelectron microscopy to estimate the amount of major basement membrane proteins per unit length and per unit area of glomerular basement membrane.

Results. Cases of IgAN showed considerably more glomerular collagenase activity than normal ($P=0.001$). Thin basement membrane disease showed no difference in collagenase activity. A count of LCA-positive cells in glomeruli confirmed that the IgAN cases did not show glomerular leukocyte infiltration. Conversely, cases of IgAN showed no difference in GBM composition from normal, nor was any difference in GBM thickness detected in this group. However, cases of TBMD showed considerably less laminin ($P=0.0008$), fibronectin ($P=0.002$) and type VI collagen ($P=0.0005$) per unit length of basement membrane. Collagen IV showed a smaller reduction per unit length ($P=0.01$), but unlike the other protein studies it appeared to be present in higher concentration per unit area ($P=0.03$), suggesting that it is more ‘compact’ in TBMD disease.

Conclusions. Two distinct mechanisms of haematuria seem to be involved in these two conditions. In IgAN there is increased activity of enzymes that can degrade

GBM, probably reflecting mesangial cell activation. In TBMD an abnormal composition of the thinned GBM is confirmed. When considered with published reports of genetic abnormalities in TBMD, these results raise the possibility of an abnormal interaction between collagen IV and laminin.

Keywords: IgA nephropathy; immunoelectron microscopy; thin basement membrane disease; type IV collagen; zymography

Introduction

Glomerular disease often causes haematuria. In such cases erythrocytes must escape to the urinary space through the glomerular basement membrane (GBM), implying the presence of gaps in what is normally a continuous membrane.

In forms of glomerulonephritis with leukocytes infiltrating the glomeruli, the presence of basement membrane defects can be explained readily, as the normal function of inflammatory cells requires them to penetrate vascular basement membranes to achieve exocytosis. They can produce inflammatory mediators, reactive oxygen products [1] and several types of proteinases, such as MMP1, MMP2, MMP3 and MMP9 [2–4]. They express membrane-type metalloproteinases (MT-MMPs) on their surface [5]. These substances have the ability to damage GBM matrix structure and may be expected to produce haematuria.

However, several forms of glomerular disease that are clinically characterized by haematuria lack significant leukocyte involvement—such as mild cases of IgA nephropathy (IgAN) and thin basement membrane disease (TBMD), which are the commonest causes of isolated microscopic haematuria in young people [6]. The activity of leukocytes cannot readily explain glomerular injury and haematuria in these conditions. The presence of infrequent GBM defects has been confirmed in IgAN using scanning electron

Correspondence and offprint requests to: Dr P. N. Furness, Department of Pathology, Leicester General Hospital, Gwendolen Road, Leicester LE5 4PW, UK. Email: pnf1@le.ac.uk

microscopy [7] and recently in TBMD using transmission electron microscopy [8]. However, the pathogenesis of these defects is not understood. In TBMD it is assumed that the molecular composition of the GBM is abnormal, leading to 'weakness'. In some kindreds various abnormalities in the genes for collagen IV have been described [9,10], but it is clear that as with Alport syndrome [11], several different mutations in several different genes can cause the same phenotype. Indeed, there appears to be some genetic overlap between TBMD and Alport syndrome [10], though in TBMD the complete absence of the $\alpha 3-5$ chains of collagen IV cannot be demonstrated. The possibility that other basement membrane proteins could be involved in some kindreds has not been excluded.

In mild IgAN, without detectable glomerular infiltration by leukocytes, the explanation of haematuria is perhaps even more elusive. All the intrinsic glomerular cells have been shown to be capable of producing type IV collagenases *in vitro*, under the control of a variety of cytokines, including IL-1, TNF and TGF- β 1 [12–15]. However, in histologically mild IgAN the morphological changes are confined to the mesangium and the peripheral glomerular capillary loops appear entirely normal on electron microscopy.

Our initial hypothesis was that, if defects occur in the GBM in the absence of infiltrating leukocytes, either there must be an abnormality of the composition of the GBM, making it abnormally weak, or there must be localized enzymatic dissolution of the GBM from a source other than inflammatory cells. In TBMD the assumption is that the composition is abnormal, but the nature of the abnormality is unknown. In IgAN the occasional observation of an abnormally thin GBM suggests that its composition may be abnormal, but this possibility has not been investigated.

We have used quantitative immunoelectron microscopy to assess changes in the amount of the major structural GBM proteins in these two conditions. We used quantitative *in situ* zymography to estimate levels of activity of glomerular gelatinase activity, to test the alternative hypothesis that defects might be due to excess degradation. The absence of infiltrating leukocytes was confirmed by immunohistochemistry.

Subjects and methods

Patients

Biopsies linked to a diagnosis of TBMD, IgAN and 'normal' were selected from the archives of the Department of Pathology at Leicester General Hospital, which has a long history of using renal biopsy to investigate microscopic haematuria even with normal renal function [6]. The 'normal' cases had presented with isolated microscopic haematuria but no proteinuria and showed no pathological findings by light microscopy, electron microscopy, and immunohistochemistry for immunoglobulins and complement. The initial diagnosis of thin membrane nephropathy was made on the

basis of a relatively limited number of direct measurements of basement membrane thickness. The diagnosis of IgAN was made on the basis of conventional criteria, including the demonstration of predominant IgA in the mesangium of all glomeruli and mesangial electron dense deposits on electron microscopy. Cases were excluded if there was a nephrotic presentation, acute renal failure or obvious inflammatory cell infiltration by light microscopy. Consequently, the IgAN cases either showed a mild increase in mesangial cellularity (segmental or global) or appeared normal by light microscopy (Haas class I or II [16]). Cases were also excluded if a snap-frozen sample containing glomeruli was not available in the archive.

Preliminary studies [17] indicated that the reproducibility of the measurements was relatively poor, for both immunoelectron microscopy and *in situ* zymography, but reproducibility was improved if samples for comparison were processed as a batch rather than sequentially. It was physically impossible to process all the biopsies in one batch, so cases were grouped into 'triplets'. Each triplet contained one case of TBMD, one IgAN and one normal. The cases in each triplet group were closely matched for patient age, gender and the time the biopsies had spent in the liquid nitrogen store (although subsequent analysis failed to demonstrate any detectable effect from these factors—data not included). Each triplet was handled as a single batch throughout the processing steps, thus, permitting statistical testing of the results from 'paired' samples.

In situ zymography protocol

The principle of *in situ* zymography has been described elsewhere [18]. In brief, any gelatinase activity in frozen sections will be manifest as digestion of an overlay of autoradiographic emulsion; hence, areas with enzyme activity will be bright under transmission microscopy, against a background of black emulsion. The extent of this digestion over specific structures (such as glomeruli) can be estimated by measurement of the amount of light transmitted through the structures in question. The results are expressed on an arbitrary scale, but this suffices for comparison of enzyme activity between groups. Unlike gel zymography, tissue localization is achieved, but it is impossible to know which enzyme is responsible for the digestion.

Frozen tissue sections (3 μ m) were cut on to uncoated clean glass slides. The sections were washed with PBS pH 7.3 for 5 min on a slow shaker, drained and wiped around the sections. Slides were dipped in autoradiographic emulsion (Type NTB-2, Kodak, catalogue no. 1654433), diluted 1:2 in filtered distilled water and melted in a water bath at 40°C. The slides were placed on a cold metal plate to gel for 20–30 min. They were incubated in a humidified chamber for 24 h at room temperature to permit digestion of the gelatin. The slides were then developed in Kodak D19 at dilution of 1:1 for 4 min and fixed for 5 min, with washes with distilled water between steps.

Quantitation of *in situ* zymography results

Images were captured using a Ziess Axiophot light microscope with a Cohu integrating video camera connected to a Power Macintosh computer through a Scion LG-3 framegrabber. The software programme NIH Image (freeware, written by Wayne Rasband) was used for image analysis (Figure 1). A set of NIH Image macros was written to

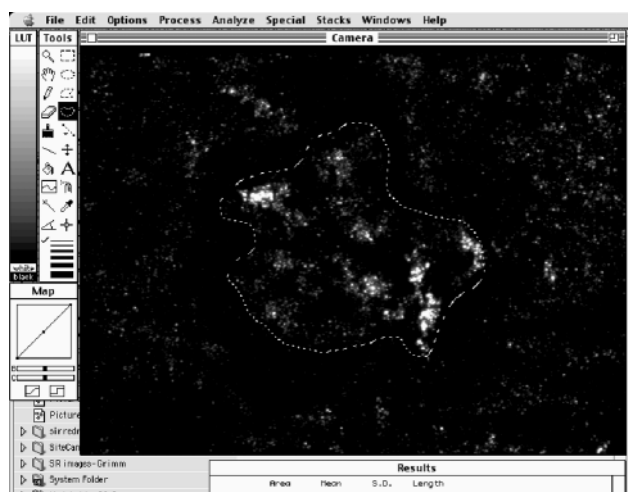


Fig. 1. Image analysis system during quantification of *in situ* zymography, with a glomerulus delineated by hand (dashed line) prior to measuring average pixel intensity.

facilitate the analysis and is freely available on request to pnf1@le.ac.uk. All available glomeruli were examined in every case (up to six). After capture of the image of a glomerulus, its outline was delineated on screen by hand and the average intensity of pixels in the selected area was measured. The result was expressed on an arbitrary scale of 0 (black; no gelatinase activity) to 255 (white; maximal gelatinase activity).

Immunoelectron microscopy

Tissue processing. The tissue remaining after *in situ* zymography was completed was fixed in freshly prepared 0.5% paraformaldehyde solution in 0.1 M PBS pH 7.3 for 2 h at 4°C and washed in several changes of PBS, then dehydrated in graded methanol (50%, 70% and 90%) at -25°C, for 45 min each step. The samples were infiltrated with LR gold monomer (Ted Pella Inc., no. 18183) at -25°C, following the manufacturer's instructions, and embedded in capped gelatin capsules filled with fresh 100% LR Gold monomer with added initiator. Polymerization was at -20°C under a projector lamp (12 V, 100 W) at a distance of 20 cm from the block for 24 h.

Selection of antibodies for immunoelectron microscopy. We initially studied a wide range of commercially available antibodies against basement membrane components and matrix metalloproteinases. Unfortunately, most proved to be unsuitable. Some did not work with the post-embedding immunoelectron microscopy method, but a common problem was that reproducibility studies [17] showed very variable results which, although morphologically relevant [18], were completely unsuited to quantitation. Pre-embedding methods were not used because of shortage of tissue and variability of results. After these preliminary studies, the only antibodies we considered suitable for quantitative work are listed in Table 1.

Post-embedding immunogold labelling. Immunolabelling was performed on ultrathin sections using a post-embedding immunogold labelling technique. Different antibodies required some modifications of the protocol, as described in Table 2.

Nickel grids with 90 nm ultrathin sections were floated face down on a drop of blocking agent (0.2% bovine serum albumin + 10% normal goat serum in PBS pH 7.3) for 10–30 min at room temperature. They were then floated on a drop of primary antibody at appropriate dilution in PBS pH 7.3 (Table 2), overnight at room temperature, or for 48 h at 4°C. Grids were washed on a drop of PBS pH 7.3 with added Tween 20, then in a few drops of PBS pH 7.3, and finally in Tris 8.2. Incubation with gold conjugated secondary antibody (particle size 10 nm) diluted in Tris buffer pH 8.2 (Table 2) was at room temperature. The grids were rinsed in Tris buffer containing Tween 20, then in distilled water, and counterstained very briefly in uranyl acetate and lead citrate.

Quantitation of immunoelectron microscopy

Image capture. The sections were examined using Philips CM100 transmission electron microscope. After screening the whole section to identify the glomeruli available for examination, areas of the peripheral capillary loops were selected at a low magnification of $\times 2500$, then photographed at $\times 11000$ subject to the following criteria: (1) peripheral GBM was selected, not areas overlying mesangium; (2) the selected areas should contain GBM excluding any area with an obviously oblique cut; (3) the grid bars were avoided by at least the width of one field; (4) each area thus selected was photographed once without overlapping; and (5) at least 10 micrographs were taken from each sample, from as many glomeruli as were available in each sample (up to six).

The electron micrographs were then printed at the same final magnification. The contrast was also matched as closely as possible for each batch of pictures to facilitate the automated image analysis.

Image analysis. The micrographs were scanned into a Power Macintosh 8100/110 computer using the Apple Color OneScanner and the Ofoto software programme at a constant setting (greyscale scan, 150 dpi).

The images obtained were analysed using the public domain program NIH image for Apple Macintosh. For each image, the area occupied by the basement membrane was delineated manually on screen (Figure 2). A set of NIH-Image macros was written to automate the required image analysis functions; these are freely available on request to pnf1@le.ac.uk. The macros automatically count the number of gold particles (which appear black) in the defined area; they also measure the length and area of this feature. From these measurements the number of particles per unit area of basement membrane and per unit length of basement membrane were calculated, as was the average thickness of the section of basement membrane examined (not corrected for any oblique cutting). Calibration to give the measurements in μm was performed with the aid of a printed micron bar on the electron micrographs.

Assessment of glomerular leukocytes

To confirm that the cases of IgAN did not contain a glomerular infiltrate of leukocytes, sections were cut from the corresponding formalin fixed, paraffin embedded tissue from each case. Immunolabelling for leukocyte common antigen (CD45, Dako) was performed using a routine indirect immunoperoxidase technique. Positive cells were

Table 1. Antibodies used in the study and their source

	Antibody	Source	Catalogue no.
Primary antibodies	Mouse anti-human collagen type IV	Dako	M 785
	Rabbit anti-laminin	Dako	Z 0097
	Rabbit anti-human fibronectin	Dako	A 0245
	Mouse anti-human collagen VI	Calbiochem	CP 22
Gold conjugated IgG	Goat anti-mouse	British Biocell	EM. GAM10
	Goat anti-rabbit	British Biocell	EM. GAR10

Table 2. Immunogold labelling conditions

GBM component	Primary Ab dilution/ incubation time, temperature	IgG gold conjugate dilution/incubation time	Special protocols
Collagen IV	1:10/48 h, 4°C	1:10/2 h	Primary Ab diluted in Tris HCl pH 7.3
Laminin	1:30/overnight, RT	1:30/2 h	
Fibronectin	1:20/overnight, RT	1:30/2 h	No blocking step
Collagen VI	1:20/overnight, RT	1:70/2 h	

Ab, antibody; RT, room temperature.

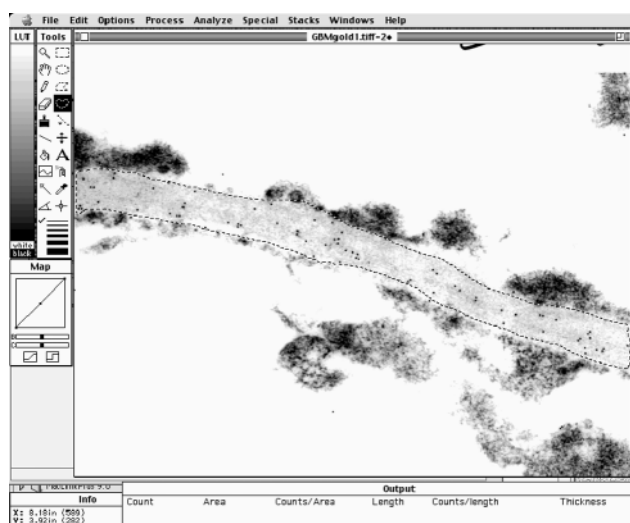


Fig. 2. Appearance of computer screen showing image analysis system during semi-automated gold particle counting. Type IV collagen is illustrated. The system reliably counts the black particles overlying the basement membrane, which has been delineated by hand. The area and mean length of the basement membrane in the image is also measured, and the mean thickness is calculated from these results (see text).

counted manually in all glomeruli and the average number of positive cells per glomerular cross-section was calculated for each case.

Statistical analysis

Calculations were carried out using the Microsoft Excel 'analysis toolpack' and the Minitab statistical package. The results for *in situ* zymography and immunoelectron microscopy were expressed as the mean value \pm 95% confidence limit for each study group. Comparison between

disease groups and normal was done using the paired *t*-test after appropriate checks confirmed an approximately normal distribution.

However, 'normal' and 'TBMD' are known to have a continuous range of thickness rather than representing two completely separate entities [19]. The measurements of GBM thickness made in this study were considerably more thorough than those on which the original diagnosis had been made. Repeating the photography and thickness measurement showed the result to be highly reproducible [17]. These measurements were not corrected for oblique sectioning and, therefore, cannot be taken as a 'true' measurement of GBM thickness, but as all study groups had been treated in exactly the same way, the measurements could be used for comparisons between the groups. Consequently, for immunoelectron microscopy a second analysis was carried out, pooling the groups and using linear regression to compare measured thickness of GBM with immunolabelling particle density. In this analysis information was lost by abandoning the separation into 'triplets', but information was gained by using the actual measured GBM thickness of each case rather than accepting the prior diagnosis and ignoring the variation within each diagnostic group.

Results

Quantitative immunoelectron microscopy

The measured 'thicknesses' of the GBMs did not vary between the control and the IgAN groups (0.24 ± 0.006 vs 0.25 ± 0.014 μ m), but the TBMD group had much thinner basement membranes (0.16 ± 0.016 μ m).

The intensity of gold particle labelling of the basement membrane was expressed in two different ways [20]. First, the total number of particles overlying a slice of basement membrane was determined. This was divided by the length of basement membrane

Table 3. Immunolabelling results of triplet groups

GBM components	Particle count/m ² area of GBM (mean + 95% confidence)			Particle count/m length of GBM (mean + 95% confidence)		
	Normal (n = 14)	TBMD (n = 14)	IgAN (n = 14)	Normal (n = 14)	TBMD (n = 14)	IgAN (n = 14)
Collagen IV	19.1 + 4.06	24.1 + 3.9 (-)	18.5 + 3.28 (-)	4.3 + 1.02	3.6 + 0.61 (-)	4.6 + 0.82 (-)
Laminin	39.4 + 10.6	31.5 + 10.74 (-)	39.8 + 7.24 (-)	9.3 + 2.18	4.7 + 1.5 (***)	10.5 + 2.37 (-)
Fibronectin	17.3 + 3.67	17.2 + 5.4 (-)	19.3 + 6.04 (-)	3.7 + 0.6	2.5 + 0.8 (*)	4.6 + 2.04 (-)
Collagen VI	71.3 + 14.78	78.0 + 11.23 (-)	75.0 + 12.05 (-)	16.9 + 4.01	14.3 + 2.91 (-)	19.8 + 4.42 (-)

Paired *t*-test, *P* value vs normal group: (-) *P* > 0.05, (*) *P* = 0.03, (***) *P* = 0.001.

examined to give the 'particles per unit length'. When the results were averaged for all measurements on a single case, as overall glomerular size is not altered we take 'particles per unit length' to be a representation of the total amount of the molecule in question in the glomerulus.

We also used the measured area of the basement membrane slices to calculate 'number of particles per unit area'. We assume this to be proportional to the 'concentration' of the protein in question in the basement membrane. We made no attempt to count particles at different levels of the basement membrane.

Thus, if basement membranes are abnormally thin simply because of a decrease in the total amount of the molecule, 'particles per unit length' would be reduced, but 'particles per unit area' would be unchanged. If a molecule is reduced in concentration, 'particles per unit area' would be decreased. If removal of one molecule led thinner membranes to have other molecules present at higher concentrations, one would expect 'particles per unit area' to be increased.

The quantitative immunoelectron microscopy results are summarized in Table 3. There were no significant differences between IgAN and normal for any of the proteins studied.

For collagen IV the TBMD group demonstrated a slightly higher mean gold particle count per GBM area and a slightly lower count per unit length when compared with the normal group, but neither measurement reached statistical significance (*P* = 0.062 and 0.23, respectively). However, when the results were correlated with the measured basement membrane thicknesses, rather than relying on the original diagnosis, statistically significant differences were found. The thinner GBM contained more gold particles per unit area but fewer per unit length than the thicker GBM. The relationship is fairly weak (*r* = 0.3 and 0.3), but it is statistically significant (*P* = 0.03 and 0.01, respectively).

This implies that thicker GBMs contain slightly more total collagen, but it is present at lower concentration; in thinner membranes the collagen present appears to be more compact.

In contrast, the mean immunogold label for laminin per GBM area of TBMD cases was slightly lower than the normal group, though the difference did not reach

statistical significance (*P* = 0.1). The laminin immunolabelling density per GBM length in the TBMD group was considerably reduced, being approximately half the value recorded for the normal group (*P* = 0.001) (Table 3). Correlation of laminin immunolabelling density with measured GBM thickness confirmed this result, with no significant association when immunolabelling was expressed per GBM area (*P* = 0.9). Correlation of laminin immunolabelling per GBM length with the GBM thickness confirmed a very significant decrease (*P* = 0.0008, *r* = 0.56).

This implies a considerable decrease in the total laminin content of glomeruli in TBM disease, a decrease that is roughly proportionate to the degree of GBM thinning.

The results for fibronectin paralleled those for laminin, with less immunolabelling per GBM length in the TBMD group (*P* = 0.03) and a positive correlation with the thickness of GBM (*P* = 0.002).

The results for collagen VI immunolabelling also paralleled those for laminin. When analysed in the triplet groups a significant difference was not detected, but there was a strong correlation between immunolabelling per GBM length and measured GBM thickness (*P* = 0.00005).

In situ zymography results

The intensity of gelatinolytic activity of glomeruli in the IgAN group was considerably higher than that of the normal group (*P* = 0.001; Table 4) and the TBMD group (*P* = 0.04). The technique of *in situ* zymography provides relatively limited spatial resolution, but most of the gelatinolytic activity appeared to be over the glomerular mesangium (Figure 1). Capillary loops, Bowman's capsule and renal tubules showed much lower activity.

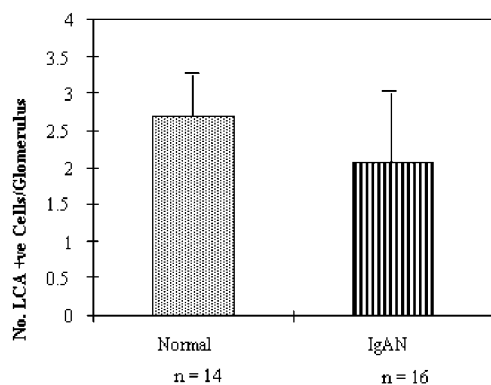
The mean intensity of glomerular gelatinolytic activity of the TBMD group was not statistically significant different from controls (*P* = 0.25).

Immunolabelling for leukocyte common antigen

Results of the LCA positive cell count in the normal and IgA nephropathy group are shown in Figure 3.

Table 4. *In situ* zymography results: intensity of gelatinolytic activity in the triplet groups

	Normal (n = 17)	TBMD (n = 17)	IgA (n = 17)
Gelatinolytic activity/glomerular area (mean + 95% confidence. Arbitrary units, scale 0–255)	64.33 + 11.9	75.78 + 15.3	106.58 + 17.5
Paired <i>t</i> -test: <i>P</i> value (vs normal)	–	0.25	0.001

**Fig. 3.** LCA positive cells per glomerulus in normal and IgAN cases. Error bars indicate 95% confidence limits.

There is no evidence of leukocyte infiltration in the glomeruli of the IgAN cases.

Discussion

If renal biopsy is used to investigate patients with isolated microscopic haematuria and normal renal function, the commonest diagnoses are mild IgAN and TBMD, conditions that usually cannot be distinguished without renal biopsy [6]. We have investigated the glomeruli in these two conditions, to investigate basement membrane composition and level of type IV collagenase activity, and we have produced very different findings in the two conditions.

In IgAN, despite reports that the basement membranes may be abnormally thin, we found no evidence of any change in the amount or distribution of the major basement membrane components that we were able to study. In these mild cases there was also no evidence of basement membrane thinning. We did, however, find a very significant increase in the level of gelatolytic activity over the glomeruli.

This result produces several questions: which enzymes are causing it, which cells are producing it, and why?

Gelatinase activity is usually assumed to relate to the two enzymes that are mainly responsible for the degradation of type IV collagen, MMP2 and MMP9, although other metalloproteinases may have significant gelatolytic effects [21]. MMP2 and MMP9 are known to be present in normal human glomeruli [18].

Unfortunately, the method of *in situ* zymography does not permit identification of the enzyme responsible.

These enzymes can be produced by circulating leukocytes and (*in vitro*) by all the three main intrinsic glomerular cell types. We have demonstrated that glomerular leukocytes were not increased in number over controls in the samples we studied, which suggests that leukocytes are not responsible. The few leukocytes present could be more active. It has been reported that monocytes from the peripheral blood of IgAN patients have higher levels of MMP9 mRNA compared with similar cells from normal individuals [22] and *in vitro* monocytes can be activated by IgA molecules *via* cell surface receptors for IgA [23]. It might be possible to investigate this further using more specific markers of leukocyte activation, but we suggest that the absence of any recruitment of leukocytes to the glomeruli makes this mechanism unlikely. The most plausible explanation is that the extracellular deposits of IgA in the mesangium are having an effect on the adjacent mesangial cells. Mesangial cells *in vitro* bind IgA complexes, either through Fc α receptors [24,25] or by other mechanisms [26]. Activated mesangial cells, as seen in experimental IgAN, increase their production of MMPs [27–29]. Moreover, the active form of MMP2 has been reported to influence the activity of mesangial cells [30]; specific inhibition of MMP2 activity resulted in a decrease of mesangial cell activation *in vitro* [31]. It remains a little difficult to explain how cells in the mesangium can digest peripheral glomerular capillary basement membrane. The *in situ* zymography did suggest maximal enzyme activity to be over the mesangium (Figure 1), but it does not have the resolution to determine the location of enzyme activity within the glomerulus with complete confidence, so other possibilities should be considered. Endothelial cells about the mesangium and can produce some MMPs [13]. In some cases of IgAN a few sub-epithelial deposits are seen, and these could perhaps influence the activity of podocytes [12], but sub-epithelial deposits are very rarely seen in the milder cases of the disease such as those we studied, and indeed we saw none during the systematic immunoelectron microscopic examination. It might be possible to investigate this further using immunohistochemistry or *in situ* hybridization, but such methods take no account of the extent of activation of the proenzyme, nor are they subject to reliable quantification. On the evidence available, we suggest that mesangial cell activation is the most likely explanation.

Thin basement membrane disease in contrast showed no change in gelatolytic activity, but changes in basement membrane composition were detected. These implied that the type IV collagen in the thin basement membrane was slightly more compact, but all the other components that we were able to study were present in considerably reduced amounts, at least proportionate to the extent of GMB thinning. The impression from these results is of a basement membrane with a near-normal 'scaffold' of type IV collagen, but a 'scaffold' that has partly 'collapsed' because many of the intervening non-collagenous molecules are missing.

The genetic cause of TBMD is poorly understood, but it is clearly a heterogeneous condition. In some kindreds it is associated with alterations in the gene for the $\alpha 4$ gene of type IV collagen [9]. Other mutations in this gene are known to be responsible for some cases of autosomal recessive Alport syndrome [11]. Thinning of the GBM is an early feature of Alport syndrome, which has led to suggestions that TBMD represents the 'carrier' state or 'forme fruste' of autosomal recessive Alport syndrome. However, TBMD, like Alport syndrome, appears to be genetically heterogeneous. Haematuria in TBMD was found to segregate with known loci for Alport syndrome (collagen IV $\alpha 3$ or $\alpha 4$) in 55% of kindreds in a recent Australian study [32], but no link was found in the other 45%. In some cases of TBMD mutations of $\alpha 3$ and $\alpha 4$ have been effectively excluded [33,34] and the condition is not sex-linked, which effectively excludes the $\alpha 5$ gene. So what is causing the abnormality?

If we follow the example of Alport syndrome, we may suggest that in TBMD a variety of genetic changes may produce a common phenotype by interfering with the molecular auto-assembly of the basement membrane. Since abnormal $\alpha 3$ can produce TBMD in some cases, we should ask what molecules interact with this molecule during assembly? Our results for collagen IV imply that total collagen IV is slightly reduced in TBMD, but that which is present is in a more compact arrangement. This could be explained by a reduction in other basement membrane components with which the collagen IV is normally connected—such as laminin. Our finding of particularly low levels of laminin in TBMD hints at the possibility that this interaction between collagen and laminin is being disrupted, perhaps by an abnormality in either molecule. However, in none of our cases was laminin completely absent from the GBM, and other molecules (notably nidogen) are known to be involved in the self-assembly process. It is of course unfortunate that because of inconsistent immunostaining we were unable to employ a wider battery of antibodies against basement membrane components, especially against nidogen, laminin subtypes and the various α chains of type IV collagen.

Our results do not provide an explanation of the mechanism of haematuria in TBMD, beyond the original assumption that the thinner basement membranes are abnormally weak. However, they do suggest

that—as in Alport syndrome—the underlying genetic abnormality causes a defect in assembly which influences incorporation of several molecules in addition to the one that harbours the genetic defect.

In summary, we have demonstrated increased glomerular gelatolytic activity, probably arising from activated mesangial cells, in mild IgAN but not in TBMD. In TBMD we found type IV collagen in the GBM to be more compact, while the other basement membrane components examined (especially laminin) were reduced, but not absent. Our results indicate different mechanisms of microscopic haematuria in these two conditions and provide suggestions for the direction of future study.

Acknowledgements. This work was supported by the Joint Supervision Programme of King Abdulaziz University, Jeddah. Much of the material presented here represents work from the doctoral thesis of S. M. Jalalah.

References

1. Johnson RJ, Guggenheim SJ, Klebanoff SJ *et al.* Morphologic correlates of glomerular oxidant injury induced by the myeloperoxidase-hydrogen peroxide-halide system of the neutrophil. *Lab Invest* 1988; 58: 294–301
2. Johnson RJ, Couser WG, Alpers CE *et al.* The human neutrophil serine proteinases, elastase and cathepsin G, can mediate glomerular injury *in vivo*. *J Exp Med* 1988; 168: 1169–1174
3. Goetzl EJ, Banda MJ, Leppert D. Matrix metalloproteinases in immunity. *J Immunol* 1996; 156: 1–4
4. Vissers MC, Winterbourn CC. Gelatinase contributes to the degradation of glomerular basement membrane collagen by human neutrophils. *Coll Relat Res* 1988; 8: 113–122
5. Pei D. Leukolysin/MMP25/Mt6-MMP: a novel matrix metalloproteinase specifically expressed in the leukocyte lineage. *Cell Res* 1999; 9: 291–303
6. Topham PS, Harper SJ, Furness PN *et al.* Glomerular disease as a cause of isolated microscopic haematuria. *Q J Med* 1994; 87: 329–335
7. Nishimura S, Makino H, Ota Z. Three-dimensional ultrastructural changes of acellular glomerular basement membrane in various types of human glomerulonephritis. *Nephron* 1989; 53: 9–17
8. Collar JE, Ladva S, Cairns TD, Cattell V. Red cell traverse through thin glomerular basement membranes. *Kidney Int* 2001; 59: 2069–2072
9. Lemmink HH, Nillesen WN, Mochizuki T *et al.* Benign familial hematuria due to mutation of the type IV collagen $\alpha 4$ gene. *J Clin Invest* 1996; 98: 1114–1118
10. Buzza M, Wang YY, Dagher H *et al.* COL4A4 mutation in thin basement membrane disease previously described in Alport syndrome. *Kidney Int* 2001; 60: 480–483
11. Tryggvason K, Zhou J, Hostikka SL, Shows TB. Molecular genetics of Alport syndrome. *Kidney Int* 1993; 43: 38–44
12. Knowlden J, Martin J, Davies M, Williams JD. Metalloproteinase generation by human glomerular epithelial cells. *Kidney Int* 1995; 47: 1682–1689
13. Lenz O, Striker LJ, Jacot TA *et al.* Glomerular endothelial cells synthesize collagens but little gelatinase A and B. *J Am Soc Nephrol* 1998; 9: 2040–2047
14. Baricos W, Cortez SL, El-Dahr SS, Shnaper HW. ECM degradation by cultured human mesangial cells is mediated by a PA/plasmin/MMP-2 cascade. *Kidney Int* 1995; 47: 1039–1047
15. Martin J, Knowlden J, Davies M, Williams JD. Identification and independent regulation of human mesangial cell metalloproteinases. *Kidney Int* 1994; 46: 877–885

16. Haas M. Histologic subclassification of IgA nephropathy: a clinicopathologic study of 244 cases. *Am J Kidney Dis* 1997; 29: 829–842
17. Jalalah SM. Glomerular changes in microscopic haematuria, studied by quantitative immuno-electron microscopy and *in situ* zymography. Ph.D. Thesis, 2000. Department of Pathology, University of Leicester
18. Jalalah SM, Furness PN, Barker G *et al*. Inactive matrix metalloproteinase 2 is a normal constituent of human glomerular basement membrane. An immuno-electron microscopic study. *J Pathol* 2000; 191: 61–66
19. Dische FE. Measurement of glomerular basement membrane thickness and its application to the diagnosis of thin basement membrane nephropathy. *Arch Pathol Lab Med* 1992; 116: 43–49
20. Slot J, Posthuma G, Chang L-Y, Crapo J, Geuze H. Quantitative assessment of immuno-gold labeling in cryosection. In: Verkleij A, Leunissen J, eds. *Immuno-gold Labeling in Cell Biology*. CRC Press, Boca Raton, Florida, 1989; 135–155
21. Stone AL, Kroeger M, Sang QX. Structure–function analysis of the ADAM family of disintegrin-like and metalloproteinase-containing proteins (review). *J Protein Chem* 1999; 18: 447–465
22. Koide H, Nakamura T, Ebihara I, Tomino Y. Increased mRNA expression of metalloproteinase-9 in peripheral blood monocytes from patients with immunoglobulin A nephropathy. *Am J Kidney Dis* 1996; 28: 32–39
23. Padeh S, Jaffe CL, Passwell JH. Activation of human monocytes via their IgA receptors. *Immunology* 1991; 72: 188–193
24. Suzuki Y, Ra C, Saito K *et al*. Expression and physical association of Fc alpha receptor and Fc receptor gamma chain in human mesangial cells. *Nephrol Dial Transplant* 1999; 14: 1117–1123
25. Barratt J, Greer MR, Pawluczyk IZA *et al*. Identification of a novel Fc α receptor expressed by human mesangial cells. *Kidney Int* 2000; 57: 1936–1948
26. Diven SC, Caffisch CR, Hammond DK *et al*. IgA induced activation of human mesangial cells: independent of Fc γ R1 (CD89). *Kidney Int* 1998; 54: 837–847
27. Hayashi K, Osada S, Shofuda K *et al*. Enhanced expression of membrane type-1 matrix metalloproteinase in mesangial proliferative glomerulonephritis. *Am J Soc Nephrol* 1998; 9: 2262–2271
28. Harendza SG, Behrens U, Zahner G, Schneider A, Stahl RA. *In vitro* characterization of the mesangial phenotype in a proliferative glomerulonephritis of the rat. *Nephrol Dial Transplant* 1997; 12: 2537–2541
29. Lovett DH, Johnson RJ, Marti HP, Davies M, Couser WG. Structural characterization of the mesangial cell type IV collagenase and enhanced expression in a model of immune complex-mediated glomerulonephritis. *Am J Pathol* 1992; 141: 85–98
30. Turck J, Pollock AS, Lovett DH. Gelatinase A is a glomerular mesangial cell growth and differentiation factor. *Kidney Int* 1997; 51: 1397–1400
31. Turck J, Pollock AS, Lee LK, Marti H-P, Lovett DH. Matrix metalloproteinase 2 (gelatinase A) regulates glomerular mesangial cell proliferation and differentiation. *J Biol Chem* 1996; 271: 15074–15083
32. Buzza M, Wilson D, Savige J. Segregation of hematuria in thin basement membrane disease with haplotypes at the loci for Alport syndrome. *Kidney Int* 2001; 59: 1670–1676
33. Piccini M, Casari G, Zhou J *et al*. Evidence for genetic heterogeneity in benign familial hematuria. *Am J Nephrol* 1999; 19: 464–467
34. Yamazaki J, Nakagawa Y, Saito A *et al*. No linkage to the *COL4A3* gene locus in Japanese thin basement membrane disease families. *Nephrol* 1995; 1: 315–321

Received for publication: 23.10.01

Accepted in revised form: 16.4.02